

## MONITORING OF RICE IN SMALL PADDY FIELDS USING MULTI-TEMPORAL SENTINEL-1 DATA

Ritche U. Nuevo  
College of Technology and Engineering  
Cebu Technological University – Argao Campus  
Lamacan, Argao, Cebu, Philippines  
and  
College of Engineering and Agro-Industrial Technologies  
University of the Philippines Los Baños  
College, Los Baños, Laguna, Philippines  
Email: ritche.nuevo@gmail.com or runuevo@up.edu.ph  
Contact Nos.: +63 932 720 8010 or +63 032 485 8024

Ronaldo B. Saludes  
College of Engineering and Agro-Industrial Technologies  
University of the Philippines Los Baños  
College, Los Baños, Laguna, Philippines  
Email: rbsaludes@up.edu.ph

Moises A. Dorado  
College of Engineering and Agro-Industrial Technologies  
University of the Philippines Los Baños  
College, Los Baños, Laguna, Philippines  
Email: madorado@up.edu.ph

Nathaniel C. Bantayan  
College of Forestry and Natural Resources  
University of the Philippines Los Baños  
College, Los Baños, Laguna, Philippines  
Email: ncbantayan@up.edu.ph

**KEY WORDS:** Synthetic aperture radar, Backscatter, Polarimetric difference, Cebu, Philippines

### ABSTRACT

Rice is the staple food for more than half of the world's population. The prompt assessment of its conditions is critical for diagnosis and decision making especially under threats of climate change. With the recent availability of C-band synthetic aperture radar (SAR) data from Sentinel-1, a 6320-m<sup>2</sup> rice paddy field employing farmer's practice in Argao, Cebu, Philippines was monitored, such that its growth can be modeled from the satellite's backscatter readings. The multi-temporal backscatter of rice and its polarimetric difference were compared with reference surfaces. The results have shown that in terms of vertical-vertical (VV) and vertical-horizontal (VH) polarized backscatter magnitude alone, rice cannot be differentiated from the other reference surfaces. However in terms of its trend over time, rice can be identified using its unique specular signature during land preparation. The polarimetric difference (VV-VH and VH-VV) was also found to be a better metric in identifying rice areas. The results have shown that canopy height and hill diameter are highly correlated with the VH polarized backscatter with R<sup>2</sup> values equal to 0.74 and 0.65, respectively. The other biophysical parameters (i.e. number of tillers, crop height, hill diameter) measured in situ did not correlate well with backscatter and its polarimetric difference. Sentinel-1 has the potential to detect small vegetative differences at closely-located ground truth (GT) points. It is recommended that further studies be conducted in this area such that the use of Sentinel-1 as an agricultural monitoring tool be maximized.

## INTRODUCTION

Rice (*Oryza sativa*) is the staple food for more than half of the world population. More than 90% of the world's rice production and consumption is in Asia. About 80% of the world's rice is grown by small-scale farmers in low-income and developing countries and its production employs 140 million rice-farming households (FAO, 2014). In the Philippines, out of a total land area of 30 million hectares, 4.7 M ha is planted with rice and contributes 41% of crop production value at \$18.12 M in 2014 (PSA, 2015).

Timely and accurate information on rice is very important to the rice-growing and -consuming nations (IRRI, 2015). The prompt assessment of crop conditions is critical for diagnosis and decision making for precision crop management and food security, especially under recent conditions associated with climate change. In the same manner, rice biophysical parameters are the basic inputs to crop yield and condition models (Brisco and Brown, 1998) that are indispensable in crop yield forecasting.

A wide range of satellite sensors are available in the optical, thermal, and microwave spectral domains for the observation of terrestrial ecosystems. However, agricultural applications are highly demanding for advanced specifications in spatial, spectral, and temporal resolutions. Most remote sensing systems in the optical domain fail to observe rice in monsoon Asia due to frequent cloud cover. Other systems are short of being practical for yield monitoring due to its low temporal and spatial resolutions. In crop monitoring for precision farming and yield forecasting, the timely observation of plant biophysical and ecophysiological status is critical (Inoue et al., 2014).

Synthetic aperture radar (SAR) in the microwave spectral domain, has a huge potential for the timely assessment of biophysical and ecophysiological variables of rice (Ribbes & Le Toan, 1999) since it is not obstructed by cloud cover. In addition, the delineation of rice fields using SAR is relatively robust due to the unique specular features of rice fields under flooded surface conditions (Choudhury et al., 2012). With the combined use of multiple polarizations, agricultural fields can effectively be classified (Bouvet et al., 2009). Cropping systems or agricultural management practices in rice growing regions can be identified successfully from SAR observations. However, quantitative assessments of biophysical and ecophysiological plant variables using SAR signatures remains to be a challenge (Inoue et al., 2014). In fact, various studies in the past reported different results on the assessment of these parameters using different bands of SAR.

With the availability of Sentinel-1 data having a very high spatial (10 m x 10 m) and temporal (every 6 days) resolution, it has a multitude of applications even at the farm level. Sentinels-1A and -1B (collectively called Sentinel-1) are remote sensing satellites recently launched and maintained by the European Space Agency (ESA). It has a C-band SAR onboard with a center frequency of 5.405 GHz (ESA, 2013). This band of radar is particularly valuable for monitoring lowland rice environment due to its sensitivity to water and crop geometry (Choudhury et al., 2012). With the two satellites now orbiting 180° apart, Sentinel-1 can provide all-weather, day and night, global observation every six (6) days (ESA, 2013). More so, its data is downloadable free of charge based on the free, full and open data policy adopted by the Copernicus program for all Sentinel data products (ESA, 2013). Only a simple user registration is required for data access.

Various studies on monitoring rice canopies using C-band SAR have already been conducted. However, none attempted to apply it in the smallest scale possible—that at a single pixel level. Most of these studies focused on the identification and mapping of rice areas for policy and planning purposes. Other studies looked into the modeling of rice parameters using the retrieved backscatter signatures. A very similar case in point is one (Raviz et al., 2016) that mapped rice areas in Mindanao, Philippines using Sentinel-1 images as part of the Philippine Rice Information System (PRiSM) project of the Department of Agriculture (DA) and the International Rice Research Institute (IRRI). They were able to delineate the rice areas and have determined the start of season (SoS) based on the specular signature of paddy rice during land preparation. It did not however, monitor its growth and yield at the paddy field scale. Another similar study (Torbick et al., 2017) also used Sentinel-1 time series images to monitor rice across Myanmar. They found out that Sentinel-1 was able to detect rice extent, cropping calendar, inundation and cropping intensity. Although many studies exist on rice growth monitoring and modeling using SAR, particularly in Japan, China, India and Vietnam; none attempted to monitor and model its growth and yield comparing closely-located ground truth (GT) points. Remote sensing studies at this scale have more potential applications that could benefit small-holder rice farmers particularly in the Philippines. Such setup could easily be up-scaled for policy and planning purposes. As of the moment, most studies on rice remote sensing focus on large areas. This study therefore, aimed to assess the potential of using Sentinel-1 Ground Range Detected (GRD) products to monitor and model rice biophysical parameters at the paddy field scale. It examined the dual-polarized backscatter coefficient and the polarimetric difference of rice canopies and compared it with other reference surfaces over the growing period. It also looked into the relationship between the VH polarized backscatter and rice biophysical parameters at the paddy field scale.

## METHODS

A contiguous lowland irrigated rice paddy field with an area of 6320 m<sup>2</sup> was chosen as the study site. It is centrally located within a rice monoculture field that is owned and managed by different farmers (Fig. 1). The rice monoculture field has a total land area of 34.13 ha with average holding of less than a hectare. It has a flat terrain with a mean elevation of 3.8 m above mean sea level. The soil in the area is a type of hydrosol primarily from limestone. Although only one site was monitored for in situ data collection, three other nearby sites within the image frame were chosen as reference surfaces for comparison. A georeferenced Google Earth image was used to locate a grass covered ground, tree vegetation and an inland pond to represent ground, trees and water surfaces.



**Figure 1.** Study site located in Argao, Cebu, Philippines (Google Earth, 2016).

Farmer's practice was followed in the management of rice monitored in this study from October 2016 to February 2017. A small area within the study site was initially puddled and prepared for seeding. One bag of NSIC Rc214 was soaked for 24 hours to pre-germinate and then broadcasted into the prepared seedbed on 11 Oct 2016 (0 days after seeding, DAS). The rest of the study area was then puddled twice using a hand tractor with cage wheels. The whole field was agronomically flooded except the seedbed at 5 DAS. The first land preparation was done at 8 DAS and the second one 16 DAS. In both cases the field was puddled with standing water and weeds from the previous fallow period. The weeds, mostly broadleaves, were either buried in the field or disposed of elsewhere. Transplanting was done at 23 DAS right after levelling and the drawing of guide lines on the levelled field. Three to five seedlings were manually planted forming a hill at 25 cm by 25 cm apart. Manual and mechanical weeding were done occasionally to control weeds and maintain the paddy field bunds/dikes. Commercial fertilizers (Complete and Urea) were first applied at 55 DAS at a rate of 95-22-22 kg/ha. A second application of N (Urea) was given at 78 DAS at 35 kg/ha. Thereafter, foliar plant enzymes containing actinomycetes was applied twice at 73 DAS and at 81 DAS. A methomyl-based pesticide was applied once at 78 DAS to control rice earhead bugs (*Leptocorisa oratorius*). Irrigation water was applied following the local rotation schedules. The paddy fields were kept flooded although there were times wherein no standing water was observed in the field. It was still wet/muddy however for the whole cropping period even in the absence of standing water. Irrigation was discontinued on the last two weeks right before harvest. Finally, the crop was harvested manually using sickles on 16 February 2017 (128 DAS).

The rice plants were monitored every 12 days coinciding with Sentinel-1A satellite flyby. There were cases wherein data gathering was done one day ahead or one day after the satellite passes over the study area. These discrepancies however were limited to a maximum of only one day. Seven ground truth (GT) points were designated along a transect line which also lies along the major axis of the study area. This was considered sufficient for the study since there were no treatments applied and that normally, rice growth within each field is considered highly uniform with coefficients of variation (CV) of less than 10% (Inoue et al., 2014). The seven GT points located between 10-30 m

along the transect line (Fig. 2) served as replicates for the study. A fixed-distance buffer (5 m) was plotted around each point to serve as boundary. Four random hills were then chosen within each buffer zone to represent a composite sample. These sampling hills were monitored for biophysical changes like height, diameter and the number of tillers every 12 days coinciding with the satellite flyby. Height was measured to the nearest centimeter from the ground to the tip of the longest leaf (IRRI-PhilRICE, 2016) using a meter stick. The hill diameter was measured using a Vernier caliper and read up to the nearest millimeter. Hill diameter measurements were taken at 2-5 cm from the ground surface both in the presence or absence of surface water. As for the number of tillers, it was simply counted.

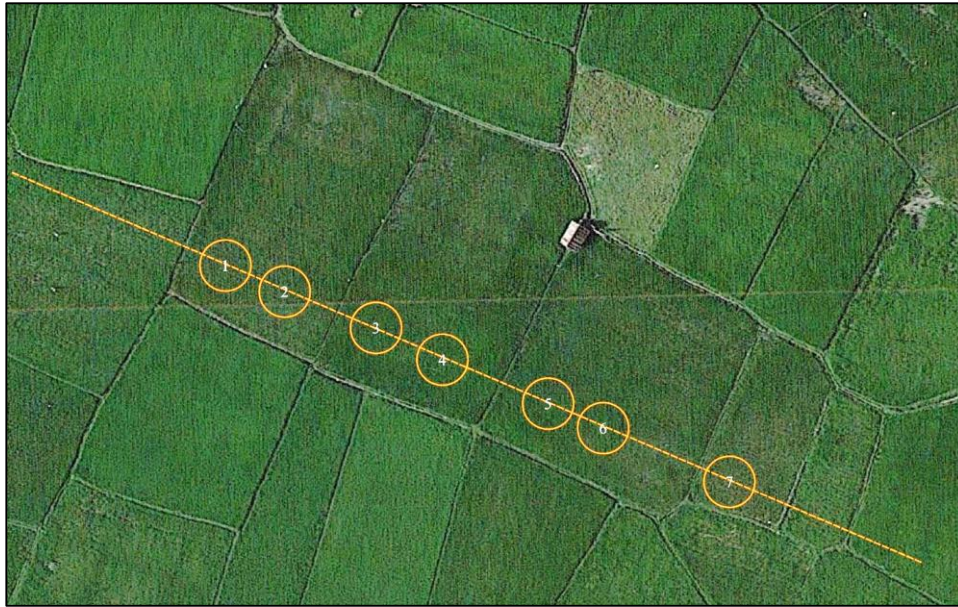


**Figure 2.** Locations of the GT points and its buffers within the study area (Google Earth, 2016)

Level-1 GRD products of Sentinels-1A and -1B were searched and downloaded from Vertex, the satellite data portal of the Alaska Satellite Facility (ASF). Using an existing NASA EarthData Distributed Active Archive Center (DAAC) account to login to ASF's Vertex mirror, the region of interest (ROI) and the inclusive period from October 2016 to February 2017 were specified as the search parameters. A detailed search was then run on the ASF's Vertex interface. The products over the ROI consistent with the search parameters were then displayed, selected and downloaded using Mozilla Firefox's DownThemAll plugin. Only three images from Sentinel-1B were available and only in the VV polarization, thus, they were eventually discarded. Only the images from Sentinel-1A were used in the succeeding analyses.

Image processing was done in the Sentinels Application Platform version 5.0 (SNAP). SNAP is a free desktop software developed by the ESA Scientific Exploration of Operational Missions (SEOM) project mainly for the processing of all Sentinel missions data of the Copernicus Program. The suggestion of Prof. Yuan Zhang, faculty of the School of Geographic Sciences at East China Normal University (pers. comm.), was followed in the processing of Sentinel-1A GRD images. First, the precise orbit files were applied to all the downloaded images. Thermal noise was then removed, then the images were calibrated. After calibration, speckle filtering was done then terrain correction. In consideration of future possible studies in the same area, image subset was done last. Finally, the subset image was then exported as GeoTIFF. All processing operations in SNAP 5.0 were done via a batch process using the graph builder. The final result was a subset image (195 x 153 pixels) focused on the ROI with 22 bands and projected in UTM Zone 51N coordinate reference system (CRS). Each band represents the multi-temporal image intensity values either in VV or VH polarization.

When the final GeoTIFF product was loaded in QGIS environment, regular points were then generated at 10 m x 10 m and with 5-m offset from the edge of the image. This process created a point at the center of each pixel. A georeferenced Google Earth image was overlaid on the ROI to find other reference surfaces for comparison. To check the accuracy of the google earth image and chosen reference points, it was compared to the coordinates taken in the field using a handheld GPS receiver. All the other regular points were deleted except the ones overlaying the study area and the chosen reference surfaces. All points within the study area were preserved. Four adjacent points were also preserved on each of the chosen known reference surfaces. A total of 78 points were left for data sampling, 66 from the monitored rice study area and four adjacent points from each of the other three reference surfaces. The sampling point tool plugin was then run to capture the backscatter values from each of the bands in the stacked image.

The newly generated shapefile was then exported to CSV format and further processed in MS Excel 2013. The data were then transposed and grouped according to polarization, date and surface type it represented. Only the intensity values from the pixels overlain by the 5-m buffer zone of the seven sampling points were used in the analysis. Pixels with less than 10% area coverage of the buffer zones were discarded. Thus, each point has a varied pixel representation of one to four. All backscatter power intensity values were then converted into decibel units using the  $\sigma^0 = 10 * \log(DN)$  conversion equation where:  $\sigma^0$  is the backscatter coefficient in decibels (dB) and DN is the digital numbers in power intensity units. Various graphs were then generated using Excel's chart function. Statistical summaries were generated using the AVERAGE and STDEV functions and the ANOVA function within the Analysis ToolPak Add-in. Linear and nonlinear regression was also done using XLSTAT add-in for MS Excel.

## RESULTS AND DISCUSSION

### Backscatter of Rice Canopies and Reference Surfaces

The VV and VH backscatter of rice canopies were compared to other reference surfaces for the cropping period. This was done to observe the unique features of rice canopy backscatter over time as mentioned in the literature. Although they have different values, VV being higher compared to VH, they follow the same trend. Meaning, when VV increases, VH also generally increased. The unique multi-temporal signature of rice in C-band SAR was observed. Both VV and VH dropped during flooding and land preparation and then increased with the increase in vegetation (Fig. 3). This particular trend was not observed in the other reference surfaces. Although both VV and VH backscatter values of rice canopies are often between that of trees and grass covered ground or water, such that one would expect that it would be difficult to detect, its dynamic range of values is higher compared to the other references surfaces particularly the VH backscatter. This is consistent with the observation of Choudhury and Chakraborty (2006) wherein rice displayed a backscatter range of -18 to -6 dB when they used Radarsat-1 images. They've noted that it has the largest dynamic range among all other land covers. In this study, rice has a range of 3.71 dB for VV and 6.27 dB for VH.

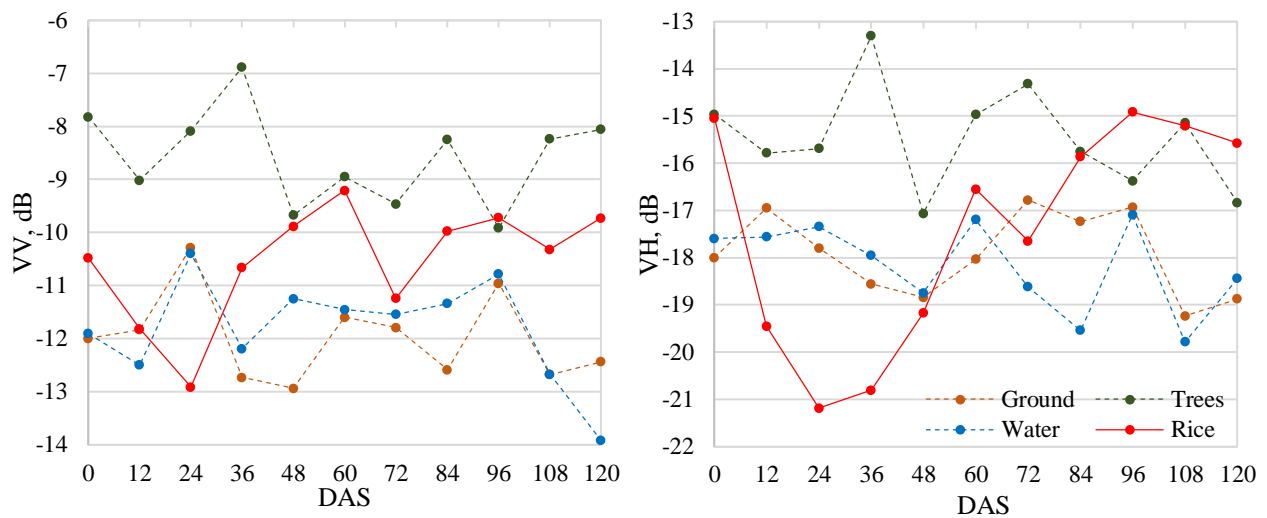


**Figure 3.** VV and VH backscatter of rice and other reference surfaces during the cropping period.

Among the reference surfaces examined, only rice showed a 3-point successive backscatter drop in the course of 36 days. Correspondingly, only rice showed a 3-point successive increase in backscatter over the course of 36 days (Fig. 3). The other known reference surfaces did not have this behavior. Such signal pattern is used as the indicator to classify and map rice fields. This particular observation is consistent with other studies like that of Chakraborty et al. (2005), Inoue et al. (2014) and Choudhury et al. (2005). This drop coincides with land preparation and agronomic flooding of the paddy fields. The same signal pattern was observed for the VH backscatter. The main difference lies in the magnitude of the backscatter signals. The VH backscatter is more attenuated compared to VV for all surfaces. The increase in backscatter signals from 36 DAS to 96 DAS is more pronounced in VH than VV.

Due to the flat surface of water bodies, they tend to scatter radar signals away from the sensor, thus it should have the least backscatter compared to the other surfaces and should be more or less constant over time. In this study, however, water had a similar signal compared to that of the grass covered ground. In fact, in most of the observation days, water had a higher backscatter compared to ground surfaces both in VV and VH. Such observation could be attributed to waves. It should be noted that the Northeast monsoon was active during the data gathering period. In a

nearby (3.2 km) Automatic Weather Station (AWS), the wind speeds recorded during the period ranged from 0.2 to 7.6 km/hr. In addition, the water surface taken as a reference surface is an inland ornamental pond. It is surrounded by trees and has a concrete statue at the center. The high backscatter readings could also be attributed to multiple volume scattering from the surrounding trees and the statue. The same reasoning can be followed for the tree vegetated surface. Considering the vertical structure of trees and the presence of branches and leaves, it is also a volume scatterer. Wind disturbance could also amplify the backscattering effect of the leaves. If only the magnitude of the backscatter of the surfaces will be used to identify and classify rice, it would be impossible since they have more or less similar values. However, if its trend is considered over time, the unique specular signature of rice can be used to effectively classify rice planted areas.

To further investigate the behavior of the backscatter of rice surfaces over the growing period, the difference in VV and VH was explored. Figure 4 below shows this difference over the growing period. As can be seen in the figure, only rice has this wide range in VV-VH difference. This suggests that both VV and VH backscatter signals from other surfaces like the ground, water and trees, are attenuated at about the same rate. In the case of rice, VH is more attenuated than the VV backscatter, thus the difference is higher. It has been pointed out in prior studies that VV polarized backscatter should be more attenuated compared to HH polarized since rice vegetative structure has a dominant vertical orientation. The results in this study do not totally contradict the results of previous studies. SAR signals were originally oriented vertically when sent out from the Sentinel-1A platform and then depolarized by rice canopies to horizontal when backscattered. The magnitude of attenuation in the VH polarization compared to VV is in fact expected since the signals were originally transmitted in the vertical direction. At 0 DAS, this difference is very small, meaning they have more or less the same value. This suggests that the broadleaf weeds present during that time attenuates both polarization at about the same rate. The backscatter difference in rice canopies clearly shows the differences in attenuation of the two polarizations and such magnitudes are not found in other surfaces. This signature can as well be used to detect rice areas in comparison to other surfaces and might in fact, result to better detection accuracies than using simply the polarized backscatter alone.

The opposite was observed when VV was subtracted from VH. The VH-VV plot is simply a mirror image of the VV-VH plot. This makes sense because the same values were used in the operation except VV is now subtracted from VH. This approach could exaggerate the lowest point during agronomic flooding and exaggerate maximum backscatter during maximum tillering period or before the first land preparation in the presence of weeds. Just as in the previous setup, this could also be a better metric in classifying rice-planted areas. The other reference surfaces do not have this characteristic. With the wide dynamic range of rice backscatter, the difference in VV and VH polarized backscatter showed a strong variation compared to the other reference surfaces.

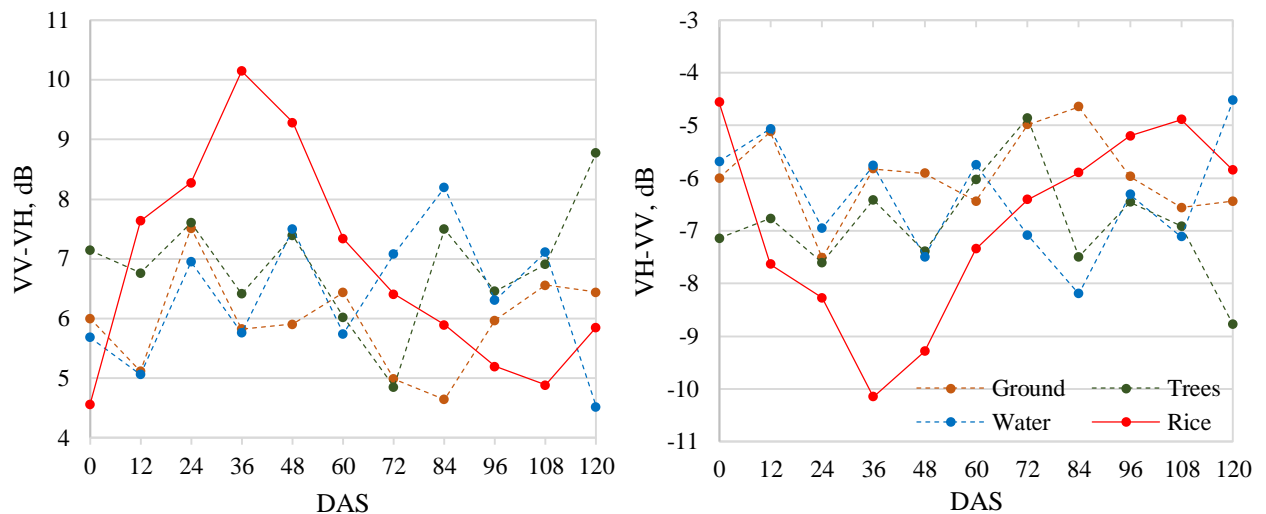
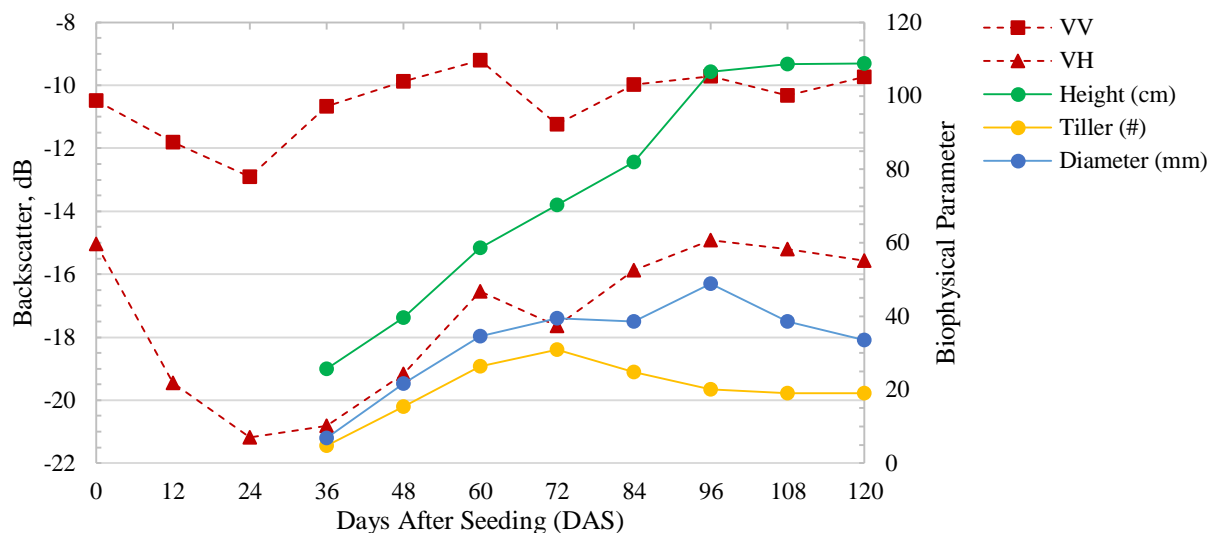


Figure 4. VV-VH and VH-VV backscatter difference over the cropping period.

### Modelling Rice Biophysical Parameters from VH Backscatter

Rice canopy height, number of tillers and hill diameter were measured starting at 36 DAS and every 12 days thereafter until 120 DAS. For the seven observation points in four replicates and eight observation days, there were a total of 224 observation pairs. The means of the four replicates was instead used, thus in the final regression analysis, there were only a total of 56 data pairs. The rice canopy height averaged 25.6 cm on 36 DAS and grew about 16 cm every 12 days until it plateaued on 96 DAS at 106.6 cm. During the maturation stage it increased only to a maximum of

108.8 cm on 120 DAS. Fig. 5 shows the vegetative parameters plotted against days. For reference purposes and to spot the similarity of trend, the VV and VH backscatter are also shown in a different axis.



**Figure 5.** Backscatter and biophysical parameters of rice over the growing period.

Based on the trends in Fig. 5 and a trial trendline analysis in MS Excel, the biophysical parameters closely relates to VH. A regression analysis was then run to express the biophysical parameters as a function of VH. In the case of canopy height, the results showed that the three models (i.e. linear, quadratic and exponential) used have similar coefficients of determination ( $R^2$ ) ranging from 0.74 to 0.76 (Table 1). For the linear model, its equation is of the form  $Y = A + BX$ , where: Y is the modeled biophysical parameter (in this case height), A is the first parameter (or intercept), B is the second parameter (or slope) and finally X is the input parameter (in this case VH). The quadratic model is of the form  $Y = A + BX + CX^2$  and finally the exponential model is of the form  $Y = Ae^{BX}$ . Such designations of parameters (i.e. A, B, and C) shall be consistently used in the succeeding analyses for the other biophysical parameters measured in situ. Finally, the test of significance for the computed parameters have shown that all the models gave highly significant results (Table 1).

**Table 1.** Summary of regression results between VH backscatter and canopy height.

Statistics	Linear Model	Quadratic Model	Exponential Model
Observations	56	56	56
$R^2$	0.74	0.76	0.75
MSE	249.66	237.61	240.70
RMSE	15.80	15.41	15.51
A	277.99	522.98	1544.62
B	11.96	39.91	0.18
C	-	0.78	-
P-value (A)	0.00**	0.00**	0.00**
P-value (B)	0.00**	0.00**	0.00**
P-value (C)	-	0.03*	-

\*\* Highly significant at  $\alpha = 0.01$ , \* Significant at  $\alpha = 0.05$ , <sup>ns</sup> Not significant

The number of tillers per hill also behaved similarly with the other vegetative parameters. On 36 DAS there were on average 4.7 tillers/hill, it then increased at about 10 tillers every 12 days until 60 DAS. The number of tillers peaked on 72 DAS at 30.8 tillers/hill on average. After that period it declined to only 19 tillers on 120 DAS. Such observation is also consistent with prior observations (Yoshida, 1981) wherein after the maximum tillering period, some of the unproductive tillers die out. Up until the maximum tillering period at about 72 DAS, the number of tillers slowly decreased until harvest. The regression results showed that the quadratic form of relationship has the highest  $R^2$  value at 0.40 and all three models gave significant results. The summary statistics are shown in Table 2.

Just as the other vegetative parameters, the hill diameter increased until 96 DAS. Rice, being an annual crop, senesces after the reproductive stage. The hill diameter increased from 6.7 mm on 36 DAS to 48.9 mm at 96 DAS. During the early vegetative stage, it grew at a rate of about 13 mm every 12 days. From its widest diameter on 96 DAS, it decreased to 33.5 mm on 120 DAS. Based on curve similarity in Fig. 5, the crop hill diameter was also paired with

VH backscatter for regression analysis. Its results showed that its best fit is a quadratic function with R<sup>2</sup> value equal to 0.67. Although the R<sup>2</sup> value is higher than that of the linear function, further statistical confirmation of the model parameters showed that the linear function has a higher significance than the quadratic function (Table 3).

**Table 2.** Summary of regression results between VH backscatter and number of tillers/hill.

Statistics	Linear Model	Quadratic Model	Exponential Model
Observations	56	56	56
R <sup>2</sup>	0.24	0.40	0.21
MSE	52.78	42.43	55.56
RMSE	7.26	6.51	7.45
A	51.06	-150.51	78.05
B	1.83	-21.17	0.08
C	-	-0.64	-
P-value (A)	0.00**	0.00**	0.01*
P-value (B)	0.00**	0.00**	0.00**
P-value (C)	-	0.00**	-

\*\* Highly significant at  $\alpha = 0.01$ , \* Significant at  $\alpha = 0.05$ , <sup>ns</sup> Not significant

**Table 3.** Summary of regression results between VH backscatter and hill diameter.

Statistics	Linear Model	Quadratic Model	Exponential Model
Observations	56	56	56
R <sup>2</sup>	0.66	0.67	0.61
MSE	57.37	56.59	65.49
RMSE	7.57	7.52	8.09
A	111.38	29.73	365.36
B	4.63	-4.68	0.14
C	-	-0.26	-
P-value (A)	0.00**	0.31 <sup>ns</sup>	0.00**
P-value (B)	0.00**	0.26 <sup>ns</sup>	0.00**
P-value (C)	-	0.09 <sup>ns</sup>	-

\*\* Highly significant at  $\alpha = 0.01$ , \* Significant at  $\alpha = 0.05$ , <sup>ns</sup> Not significant

### Differences of Parameter Values at the Pixel Level

To peer into the possible detection of rice canopy conditions at the pixel level, the sampling points that are located at least 10 m apart were compared among each other. An analysis of variance (ANOVA) of the different parameters studied (i.e. VV, VH, height, tillers and hill diameter) was run using the Analysis ToolPak Add-in of Excel. It should be noted that there were no treatments applied. The same variety (NSIC Rc214) and farmer's practice was applied to the whole study area and the different sampling points all throughout the cropping period. The four sampling hills which made up a composite sample and the four adjacent image pixels within and around the buffer, were taken as replicates. In addition, only the backscatter readings and in situ vegetative data on 120 DAS were used for this analysis.

**Table 4.** Summary of ANOVA results for all parameters tested on 120 DAS

Parameter	Mean	SD	CV	SE	F	p-value	F-crit	Remarks
VV Backscatter (dB)	-9.95	0.87	5.96	0.11	4.61	0.00	2.57	**
VH Backscatter (dB)	-15.51	1.05	3.80	0.11	8.13	0.00	2.57	**
Canopy Height (cm)	108.82	8.69	5.72	11.35	3.98	0.00	2.57	**
No. of Tillers/Hill (f)	19.00	4.15	17.73	3.02	2.91	0.03	2.57	*
Hill Diameter (mm)	33.54	4.64	11.37	4.06	2.46	0.06	2.57	ns

\*\* Highly significant at  $\alpha = 0.01$ , \* Significant at  $\alpha = 0.05$ , <sup>ns</sup> Not significant

The results have shown that the VV and VH backscatter, canopy height and the number of tillers/hill of the seven closely-located GT points are significantly different from each other. No significant difference was found for hill diameter (Table 4). This suggests that even with rice monoculture applied with the same farmer's cultural management practices, as long as no stringent scientific controls are in place, a single cropping could produce varying crop canopy conditions. Moreover, Sentinel-1A has enough radiometric resolution or sensitivity that it can differentiate between adjacent pixel readings. In fact, the closest plots in this study shared one or two pixels. The

relationship of the backscatter variables to the different biophysical parameters, however, are not explicitly presented here. It is beyond the scope of this study. Only a regression analysis was conducted to find empirical relationships between these variables. These observations have serious implications for small farm applications particularly in the Philippines, especially considering that Sentinel-1 images are free, can penetrate cloud cover and has a temporal resolution of six days.

## **CONCLUSIONS**

Based on the results of this study, it can be concluded that the unique specular signature of rice canopies does indeed exist. Such results are consistent with prior studies and that this can be attributed to the unique rice cultural practice of flooding and puddling of the field that signals the start of season (SoS). Water surfaces being flat, are known to be forward scatterers of radar particularly in C-band, thus having the characteristic low backscatter readings. The same signature was observed in both VV and VH polarizations. After this unique drop in backscatter, the continued rise in backscatter up to 72 days followed. This backscatter trend is the usual indicator used to classify rice areas from SAR images. Simple magnitudes of backscatter on the other hand, without looking into its multi-temporal trend, cannot be used to identify rice areas. Rice canopy backscatter in fact, have values more or less between that of tree vegetation and grass-covered ground.

The polarimetric backscatter difference looks promising in identifying rice areas. This combination highlights the difference in attenuation of these two linear polarizations. Prior studies have already established that rice, being generally upright, responds more to vertically polarized microwaves. This is most likely the reason why VH backscatter is more attenuated than VV. The difference of these two polarizations can give a better picture of the geometry of the target, in this case rice canopies. Based on its polarimetric backscatter difference and its trend over time, rice canopies are easier to detect and identify compared to using simply its known specular signature.

Regression analyses have shown that rice canopy height, number of tillers/hill and hill diameter are significantly correlated with VH backscatter. Only height and hill diameter have acceptable coefficients of determination. This result suggests that VH backscatter is indeed more responsive to volume scattering. This may seem inconsistent with other prior observations that the vertical structure of rice plants responds more to the vertically-oriented polarizations. This can be reconciled by stating that VV gets a strong backscatter and VH is more attenuated but correlates well with height. Other prior studies (Chakraborty et al., 2005) have shown that a second-order polynomial was the best model to express the relation between backscatter and canopy height.

Finally, adjacent Sentinel-1A image pixels can be very different from each other. Statistical analysis have shown that closely-located (10 to 30 m apart) GT points under the same treatment have different backscatter readings and biophysical parameters. Analysis of variance have shown that VV and VH backscatter, canopy height and the number of tillers/hill are significantly different from each other during the maturation stages (120 DAS). This implies that Sentinel-1A images may have the capability of detecting minute differences in vegetation conditions even within adjacent pixel clusters. Such sensitivity has a huge potential for future monitoring studies in rice.

## **RECOMMENDATIONS**

The suitability of Sentinel-1 data products for agricultural monitoring in the Philippines is very high. It has a huge potential for precision farming and local government policy making. It has even the potential of being used at the farm level. As of the moment, very few studies are taking advantage of this potential. Based on the experiences gained from this study, the following are recommended:

The sampling approach used in this study may not be the most appropriate. Instead of using a transect line, random plot assignment based on the actual locations of image pixels can be considered. This approach ensures that the sampling plots are within the designated pixels. If the transect line approach will be used, it should be along the cardinal directions of North-South or East-West. This way adjacent pixels are properly oriented and sampled. The number of sample hills per plot also seemed to be inadequate. Since there are more or less 1600 hills in a 100-m<sup>2</sup> pixel, sampling hills should be increased to about 100 hills per plot for proper representation of actual vegetation conditions. A similar study should also be conducted such that rice growing at different stages can be imaged simultaneously by Sentinel-1 for proper comparison. This way differences among plots are more pronounced and better correlations can be looked into.

Small area applications should be further looked into and that the proper methods be developed for this particular application. There are also other ways to express polarimetric backscatter combinations, they should be explored further. Finally, the application of Sentinel-1 to other types of land cover or surfaces must as well be explored.

## REFERENCES

- Bouvet, A., Le Toan, T., & Lam-Dao, N. (2009). Monitoring of the rice cropping system in the Mekong Delta using ENVISAT/ASAR dual polarization data. *IEEE Transactions on Geoscience and Remote Sensing*, 47, 517–526.
- Brisco, B., Brown, R.J., (1998). Agricultural applications with radar. Principles and Applications of Imaging Radars, 3rd edition. Manual of Remote Sensing, vol. 2. John Wiley and Sons, Inc., New York, pp. 381–406.
- Chakraborty, M., Manjunath, K. R., Panigrahy, S., Kundu, N., & Parihar, J. S. (2005). Rice crop parameter retrieval using multi-temporal, multi-incidence angle RADARSAT SAR data. *ISPRS Journal of Photogrammetry and Remote Sensing*, 59, 310–322.
- Choudhury, I. & Chakraborty, M., 2006, SAR signature investigation of rice crop using RADARSAT data. *International Journal of Remote Sensing*, 27, pp. 519–534.
- Choudhury, I., Chakraborty, M., Santra, S.C., & Parihar, J. S. (2012). Methodology to classify rice cultural types based on water regimes using multi-temporal RADARSAT-1 data. *International Journal of Remote Sensing*, 33, 4135–4160.
- European Space Agency. (2013). Sentinel-1 user handbook [ESA Standard Document]. European Commission, European Union.
- Food and Agriculture Organization. (2014). A regional rice strategy for sustainable food security in Asia and the Pacific (Final Ed.). Food and Agriculture Organization of the United Nations – Regional Office for Asia and the Pacific. Bangkok, Thailand.
- Inoue, Y., Sakaiya, E., & Wang, C. (2014). Remote Sensing of Environment Capability of C-band backscattering coefficients from high-resolution satellite SAR sensors to assess biophysical variables in paddy rice. *Remote Sensing of Environment*, 140, 257–266. <http://doi.org/10.1016/j.rse.2013.09.001>
- International Rice Research Institute. (2015). Satellite imagery to soon enable large-scale monitoring of Asia's rice areas. <http://irri.org/news/media-releases/satellite-imagery-to-soon-enable-large-scale-monitoring-of-asia-s-rice-areas>. Visited 25 April 2017.
- International Rice Research Institute & Philippine Rice Research Institute. (2016). Accelerating the development and adoption of next-generation rice varieties for the major ecosystems in the Philippines. Participatory Varietal Selection for the 2016 Dry Season. International Rice Research Institute and Philippine Rice Research Institute.
- Philippine Statistics Authority. (2015). Selected statistics on agriculture 2015. Quezon City, Philippines: Philippine Statistics Authority.
- Raviz, J., Laborte, A., Barbieri, M., Mabalay, M.R., Garcia, C., Bibar, J.E.A., Mabalot, P., & Gonzaga H. (2016). Mapping and monitoring rice areas in Central Luzon, Philippines using X and C-band SAR imagery. Paper presented at the 37<sup>th</sup> Asian Conference on Remote Sensing. October 2016, Colombo, Sri Lanka.
- Ribbes, F., & Le Toan, T. (1999). Rice field mapping and monitoring with RADARSAT data. *International Journal of Remote Sensing*, 20, 745–765.
- Torbick, N., Chowdhury, D., Salas, W. And Qi, J. (2017). Monitoring rice agriculture across Myanmar using time series Sentinel-1 assisted by Landsat-8 and PALSAR-2. *Remote Sens.* 2017, 9, 119; doi:10.3390/rs9020119.
- Yoshida, S. (1981). Fundamentals of rice crop science. International Rice Research Institute. Los Baños, Laguna, Philippines.